Published in final edited form as:
Adv Mater. 2011 April 26; 23(16): . doi:10.1002/adma.201004762.

Spin-Cast and Patterned Organo-Phosphonate Self-Assembled Monolayer Dielectrics on Metal Oxide Activated Si

Dr. Orb Acton,
Department of Materials Science and Engineering, Box 352120, University of Washington, Seattle, WA 98195-2120 (USA)

Daniel Hutchins,
Department of Materials Science and Engineering, Box 352120, University of Washington, Seattle, WA 98195-2120 (USA)

Dr. Líney Árnadóttir,
National ESCA and Surface Analysis Center for Biomedical Problems, Departments of Bioengineering and Chemical Engineering, Box 351750, University of Washington, Seattle, WA 98195-1750 (USA)

Dr. Tobias Weidner,
National ESCA and Surface Analysis Center for Biomedical Problems, Departments of Bioengineering and Chemical Engineering, Box 351750, University of Washington, Seattle, WA 98195-1750 (USA)

Nathan Cernetic,
Department of Materials Science and Engineering, Box 352120, University of Washington, Seattle, WA 98195-2120 (USA)

Guy G. Ting,
Department of Chemistry, Box 351700, University of Washington, Seattle, WA 98195-1700 (USA)

Dr. Tae-Wook Kim,
Department of Materials Science and Engineering, Box 352120, University of Washington, Seattle, WA 98195-2120 (USA)

Prof. David G. Castner,
National ESCA and Surface Analysis Center for Biomedical Problems, Departments of Bioengineering and Chemical Engineering, Box 351750, University of Washington, Seattle, WA 98195-1750 (USA)

Prof. Hong Ma, and
Department of Materials Science and Engineering, Box 352120, University of Washington, Seattle, WA 98195-2120 (USA)

Prof. Alex K.-Y. Jen
Department of Materials Science and Engineering, Box 352120, University of Washington, Seattle, WA 98195-2120 (USA); Department of Chemistry, Box 351700, University of Washington, Seattle, WA 98195-1700 (USA)

Alex K.-Y. Jen: ajen@u.washington.edu

Correspondence to: Alex K.-Y. Jen, ajen@u.washington.edu.

Supporting Information is available online from Wiley InterScience or from the author.

Keywords

Self-Assembly; Monolayers; Dielectrics; Patterning; Organic Field Effect Transistors

Self-assembled monolayers (SAMs) have emerged as viable candidates for controlling the surface properties of metals, semiconductors, and oxides for a wide range of applications in microelectronics, biotechnology, tribology, and nanotechnology.[1, 2] SAM modification of surfaces is of particular interest for biological-/chemical-sensing and organic/molecular electronic applications where the monolayer quality (order, orientation, uniformity, and stability) can play a dominant role in device functionality.[3, 4] Modification of oxide surfaces with organo phosphonic acid (PA)-based molecules have attracted increased interest in recent years for their moisture stability and lack of homocondensation.[5] PA molecules efficiently covalently bind to metal oxides following an acid-base condensation and coordination mechanism where acidic PA headgroups ($pK_a \sim 2$) readily react with more basic metal hydroxyl (M-OH) groups ($pK_a \sim 6$-9 for many metal oxides)[6, 7] resulting in stable P-O-M phosphonates ($\sim$30-70 kcal mol^{-1} adsorption energy[8]).[5] However, phosphonate SAM formation on SiO_2 has proven to be more difficult to achieve. For example, simple approaches to modify SiO_2 with PA molecules by immersion assembly,[9, 10] spin-casting,[11, 12] or microcontact printing (CP)[13] have resulted in PA headgroups physisorbed to SiO_2 through H-bonding ($\sim$10-20 kcal mol^{-1} bond energy)[14] or having poorly defined phosphonate coverage. This may be ascribed to silanol groups (Si-OH) being relatively acidic ($pK_a \sim 4.5$)[15] and the sensitivity of P-O-Si bond formation to hydrolysis.[5, 10] In order to form stable P-O-Si phosphonates on SiO_2, 48 hours of solid-state thermal annealing of PA films at 140 °C has been employed.[9, 16] This “long-term” processing may present a bottleneck for the integration of phosphonate SAMs into practical applications using SiO_2 substrates.

SAMs on ultrathin oxides as hybrid gate dielectrics for potential use in low-power electronic circuits represent a particularly stringent application where the monolayer quality dictates the electronic performance of circuit components such as organic thin film transistors (OTFTs).[3, 4, 17-21] Since patterning of the semiconductor channel in OTFTs is crucial for minimizing parasitic current between devices in complex circuits,[13, 22-24] SAM hybrid dielectrics should be compatible with subsequent patterning approaches for semiconductors. Additive approaches for patterning OTFTs (inkjet printing or CP)[13, 22] typically require fewer steps and less material consumption compared to subtractive patterning processes (photolithography or chemical/vapor etching[23]).[24] However, additive patterning of solution processed low-voltage OTFTs using SAM hybrid dielectrics have yet to be realized. Therefore, the development of efficient and high-throughput processing techniques for patterned phosphonate SAM hybrid dielectrics is desirable for their potential applications in low-power printed electronics.

Here we develop an efficient process to spin-cast or CP phosphonate SAMs onto SiO_2 substrate which is activated by *in-situ* generated nanoscale metal oxide layer to increase the surface reactivity for PA molecule binding. In principle, any metal oxide on which PA headgroups form phosphonates could be used to activate SiO_2, however, aluminum oxide (AlO_x) was chosen in this study for its successful use in SAM/AlO_x hybrid dielectrics.[3, 4, 18] Rapidly processed phosphonate SAMs on AlO_x/SiO_2 are shown to be covalently bound, densely-packed, and highly-ordered using complementary surface characterization techniques including atomic force microscopy (AFM), time-of-flight secondary ion mass spectrometry (TOF-SIMS), Fourier transform infrared spectroscopy (FTIR), X-ray photoelectron spectroscopy (XPS), sum-frequency generation (SFG) spectroscopy, and variable angle spectroscopic ellipsometry (VASE). The utility of this

rapid SAM processing is demonstrated by fabricating patterned solution processed sub-2V OTFTs with self-organized *n*-channel and *p*-channel active areas defined by patterned and spin-cast phosphonate SAM/AlO_x hybrid dielectrics (Fig. 1a). We employ an all-additive patterning approach driven by selective hydrophilic/hydrophobic interactions to indirectly pattern SAM dielectrics of **1** onto AlO_x regions left unmodified after CP of hydrophobic SAMs of **2** or **3** (see Fig. 1b for molecular structures). Subsequently, the surface energy contrast between patterned SAM regions of **1** and **3** provides selective placement of solution-processed semiconductors onto SAM hybrid dielectrics of **1**.

Prior to processing of PA-based molecules, Si substrates were activated with an air-plasma containing Al-ions generated by an Al-radio frequency (RF) electrode. The plasma treatment deposits a nanoscale layer of AlO_x, increases the thickness of the substrate oxide, and leaves the surface terminated with hydroxyl groups (see Supporting Information). Phosphonate SAMs were formed on plasma activated AlO_x by spin-coating or CP followed by a brief thermal annealing at 140 °C in air and subsequent solvent cleaning to remove excess physisorbed molecules. Aqueous advancing contact angles increase from <10° for plasma activated $AlO_x/SiO_2/Si$ to 91±3°, 108±3°, and 115±3° for substrates modified with spin-cast SAMs of **1**, **2**, and **3**, respectively. Even after extensive ultrasonication in polar solvents [tetrahydrofuran (THF), ethanol, water, or dimethylformamide (DMF)] the contact angles remained unchanged, indicative of chemically bound PA molecules. For comparison, spin-casting **2** onto air-plasma treated SiO_2/Si substrates without the presence of an AlO_x layer resulted in contact angles below 60° and only trace amounts of P observed by XPS, indicating that the nanoscale AlO_x layer plays a dominate role in the formation of phosphonate SAMs on SiO_2. AFM images (Fig. S2) show that the surface smoothness and uniformity of plasma activated AlO_x/SiO_2 does not change significantly after the SAM preparation (roughness <0.20 nm RMS). CP of **2** onto AlO_x using stamps having 3 m lines spaced 1 m apart resulted in commensurate SAM patterns as seen by AFM (Fig. S3) while **2** applied with flat stamps gave contact angles of 108°±3° and smooth surfaces comparable to spin-cast films.

The binding mode and surface elemental composition of spin-cast SAMs of **1** and **2** onto AlO_x was determined by TOF-SIMS, FTIR, and XPS. TOF-SIMS data shows the presences of covalently bound phosphonates to AlO_x (Fig. 2a and Table S1). In both negative and positive spectra for SAMs of **1** and **2**, peaks were detected consistent with PA molecules bonded to AlO_x through P-O-Al linkages, such as: $AlPO_3^-$, 105.94; found, 105.94 and $AlPO^+$, 73.95; found, 73.96. In addition, bound molecules are clearly present in spectra of SAMs from **2** as indicated by ion peaks of $[\mathbf{2}\text{-H}]^-$ calcd for $C_{18}H_{38}PO_3^-$, 333.26; found, 333.25, $[\mathbf{2}+AlO_2]^-$ calcd for $AlC_{18}H_{39}PO_5^-$, 393.24; found, 393.23, in good agreement with previous studies.[12,16] Similarly, for SAMs of **1**, ion peaks of bound alkyl chain fragments of $[\mathbf{1}\text{-}(C_6H_5OC_{11}H_{22})+AlH]^-$ calcd for $AlC_8H_{19}PO_4^-$, 237.08; found, 237.09, and phenyl ring fragments of $C_6H_6OC^-$, 106.04; found, 106.04, $C_6H_6OCH^-$, 107.05; found, 107.05, $C_6H_6H^+$, 79.05; found, 79.06, and $C_6H_6OH^+$, 95.05; found, 95.05. FTIR spectra in the $\delta_{P\text{-}O}$ region show that SAMs form a predominantly bidentate binding conformation to AlO_x (Fig. S5a). XPS surface composition showed the presence of C, P, O, Al, and Si as expected for intact phosphonate SAMs on AlO_x/SiO_2 (Table S2). The observed composition of SAMs of **2** with a carbon/phosphorus (C/P) ratio of 22 is in good agreement with that previously reported on AlO_x.[25] The higher C/P ratio of 27 for SAMs based on **1** is expected from a longer alkyl chain and the phenyl ring.

The SFG spectrum of SAMs of **1** show strong aromatic vibrations at 3071 cm^{-1} and 3043 cm^{-1}, indicating well-aligned terminal phenyl groups (Fig. 2b).[26] The conformational order of the alkyl chains was estimated based on the ratio of symmetric CH_3/CH_2 modes in SAMs of **2**. The spectral fits yield a ratio of 8.5 for SAMs of **2**, indicative of a highly-

ordered film.[27] A quantitative analysis of the ring modes in SAMs of **1** was performed yielding a tilt angle of $\beta \approx 30°$ and a twist angle of $\Delta \approx 79°$ for the plane of the phenoxy rings relative to the surface normal (see Supporting Information). The terminal -CH_3 group in SAMs of **2** showed a very similar orientation ($\beta \approx 26°$). The remarkable degree of orientational order of SAMs of **1** and **2** determined from SFG correlate well to that observed from FTIR (see Supporting Information). Furthermore, highly-ordered and densely packed SAMs are corroborated through VASE measurements showing that the thickness of SAMs of **1** and **2** on 4.0 nm thick AlO_x/SiO_2 are 2.5 nm and 2.0 nm, respectively. Assuming **1** and **2** are 3.0 and 2.3 nm long [as calculated in an all-trans conformation using Chem3D Ultra (CambridgeSoft)], the VASE determined thicknesses correspond with molecules in SAMs that are oriented upright and canted at angles of 34° and 30°, respectively, relative to the surface normal.

The dielectric properties of spin-cast phosphonate SAM hybrid dielectrics were assessed by leakage current density (J_{leak}) and capacitance density (C_i) characteristics of metal-insulator-p^{++}-Si devices (Au/SAM/$AlO_x/SiO_2/p^{++}$-Si). The J_{leak} characteristics are presented in Fig. 3a. Although the plasma activation changes the 1.8 nm thick native SiO_2 to 4.0 nm thick AlO_x/SiO_2 (as determined by VASE), J_{leak} at an applied voltage of 2 V is only reduced from 1×10^{-1} A cm^{-2} to 1×10^{-3} A cm^{-2}, respectively. This plasma grown AlO_x/SiO_2 is a poor quality dielectric compared to SiO_2 grown by conventional thermal oxidation.[28] Remarkably, spin-cast SAMs of **1**, which are only 2.5 nm thick on AlO_x/SiO_2, reduce J_{leak} by nearly four orders of magnitude to 2×10^{-7} A cm^{-2} at an applied voltage of 2 V and posses breakdown fields of ~14 MV cm^{-1}. In contrast, SAMs of **2** (2.0 nm thick) only reduce J_{leak} by about one order of magnitude to 7×10^{-5} A cm^{-2}. The significant reduction in J_{leak} using **1** compared to **2** is likely from a combination of a thicker corresponding SAM with a more closely packed terminal surface through phenyl-phenyl interactions (as high as 12 kcal mol^{-1}) versus CH_3-CH_3 van der Waals forces (<1.5 kcal mol^{-1}).[14] Metal deposited onto alkyl-chain SAMs has been shown to diffuse through the SAM causing filament structures[29] and electrical shorts. The interaction of phenyl-phenyl group for SAMs of **1** may reduce or block the penetration of metal through the SAM as has been observed for other SAMs with functionalized terminal groups (e.g. COOH[30] or aromatic end groups[31]). The low J_{leak} of SAM hybrid dielectrics of **1** is comparable to phenoxy-alkyl-silane-based SAM/SiO_2 hybrid dielectrics on Si[17] and other phosphonate SAM/metal oxide hybrid dielectrics.[3, 18, 19] However, here SAMs are rapidly formed simply by spin-casting in ambient conditions. Furthermore, spin-cast SAMs of **1** have slightly lower J_{leak} at an applied voltage of 2 V compared to SAMs processed by 15 h solution immersion assembly (Fig. 3a).

The C_i characteristics of spin-cast SAM hybrid dielectrics are presented in Fig. 3b. With p^{++}-Si as the semiconductor, C_i is increased when the bias is swept from positive (depletion in the semiconductor) to negative (accumulation) with respect to the metal contact. As expected, with the formation of a SAM on AlO_x/SiO_2, C_i decreases due to a larger total dielectric thickness, from a maximum of 880 nF cm^{-2} for bare AlO_x/SiO_2 to 450 nF cm^{-2} and 500 nF cm^{-2} for SAMs of **1** and **2**, respectively. The drop in C_i for bare AlO_x/SiO_2 past −0.75V suggests it has reached dielectric breakdown while the stable accumulation of C_i for SAMs of **1** is further evidence of its good dielectric properties. With the combination of spin-cast SAMs of **1** on AlO_x/SiO_2, low J_{leak}, high breakdown strength, and large C_i are achieved making this hybrid dielectric optimal for low-voltage OTFTs.

Taking advantage of the differences in surface energy of SAMs of **1** and more hydrophobic **3**, self-organized and patterned low-voltage solution processed *n*-channel and *p*-channel OTFTs were fabricated on spin-cast and patterned SAM dielectrics of **1** (see Fig. 1a for fabrication scheme, Fig. 4 for optical micrographs of devices, and Fig. S7 for step edge of

patterned semiconductor). CP of **3** compared to **2** resulted in higher-quality subsequent patterning of **1** and solution processed semiconductors, likely from the lower surface energy of **3** (*vide supra*). Patterned *p*-channel devices using 6,13-bis(triisopropyl-silylethynyl) pentacene (TIPS-Pen) and *n*-channel devices using [6,6]-phenyl-C61-butyric acid methyl ester (PCBM) showed stable switching characteristics and negligible hysteresis at sub-2V driving voltages (Fig. 4c and Fig. 4d). The leakage current (I_{gs}) is three to four orders of magnitude lower than the source to drain current (I_{ds}) confirming the good dielectric properties of spin-cast and patterned SAMs of **1**. Typical saturation field effect mobilities (, subthreshold slopes (S), threshold voltages (V_t) and on-off current ratios (I_{on}/I_{off}) were 0.02–0.11 $cm^2\ V^{-1}\ s^{-1}$, 130–100 mV dec^{-1}, −0.70–−0.90 V, and 10^5 for TIPS-Pen and 0.02–0.06 $cm^2\ V^{-1}\ s^{-1}$, 130–100 mV dec^{-1}, 0.40–0.60 V, and 10^5 for PCBM. The here for TIPS-Pen and PCBM OTFTs are comparable to previously published non-patterned high-voltage OTFTs based on the same semiconductors.[32, 33] In addition, pentacene based OTFTs were fabricated on spin-cast SAM dielectrics and showed good performance with , S, V_t, and I_{on}/I_{off} of 0.9–1.1 $cm^2\ V^{-1}\ s^{-1}$, 100 mV dec^{-1}, −0.80 V, and 10^6 (Fig. S6). We note that OTFTs fabricated on patterned bare AlO_x/SiO_2 without the spin-cast SAM dielectric all failed from dielectric breakdown due to the poor oxide quality.

In summary, we have developed an efficient process to modify SiO_2 with phosphonate SAMs by spin-casting or CP enabled by an *in-situ* generated nanoscale AlO_x activation layer. Complementary surface characterization using AFM, TOF-SIMS, FTIR, XPS, SFG, and VASE suggests that phosphonate SAMs processed on AlO_x/SiO_2 are covalently bound, densely-packed, and highly-ordered. Using these rapid SAM formation techniques, we introduced an all-additive patterning approach for SAM/metal oxide hybrid dielectrics on Si substrates which provide exceptional dielectric properties and compatible surface energy for subsequent patterning of solution processed *n*-channel and *p*-channel low-voltage OTFTs. These results provide a potential route for processing high-throughput, patterned, solution processed OTFTs for low-power electronic applications. Furthermore, we believe that activation of other technically relevant surfaces with an *in-situ* generated nanoscale metal oxides may enable efficient phosphonate SAM surface modification by rapid processing.

Experimental

Spin-cast phosphonate SAMs on plasma activated AlO_x/SiO_2

p^{++}-Si wafers were solvent cleaned, dried with N_2(g), treated with air-plasma (75 mTorr, 40 kHz, 100 W, 10 min) generated by an Al-RF electrode fixed inside the plasma chamber, then used immediately for spin-coating or CP of phosphonate SAMs. The spin-coating procedure was adapted from Nie *et al.*.[11, 12] Here, 3 mM solutions of **1** or **2** (PCI Synthesis) were dissolved in chloroform:THF (4:1, v:v) or **3** (Specific Polymers) was dissolved in chloroform:ethanol (1:2, v:v), filtered with a 0.2 n PTFE filter, dispensed onto AlO_x activated Si, left to sit for 10 sec, then spun at 3000 rpm for 20 sec. After spin-casting, substrates were baked at 140 °C on a hotplate in air for 10 min, then extensively washed with DMF:TEA (95:5, v:v), and THF or ethanol while spinning at 3000 rpm. A temperature of 140 °C was chosen for thermal annealing to facilitate the diffusion of unbound molecules[34] in the as-spun film to reorganize and form phosphonates with AlO_x.

Supplementary Material

Refer to Web version on PubMed Central for supplementary material.

Acknowledgments

This work is supported by the NSF-STC program under DMR-0120967, the AFOSR program under FA9550-09-1-0426. The authors thank J.E. Anthony (University of Kentucky) for supplying the TIPS-Pen. A. K.-Y. Jen thanks the WCU-NRF of Korea under the Ministry of Education, Science and Technology (R31-10035). T. W. thanks the Deutsche Forschungsgemeinschaft, and L.A., T.W. and D.G.C thank NIH grant EB-002027. Part of this work was conducted at the University of Washington NTUF, a member of the NSF-NNIN.

References

1. Schreiber F. Prog Surf Sci. 2000; 65:151.
2. Love JC, Estroff LA, Kriebel JK, Nuzzo RG, Whitesides GM. Chem Rev. 2005; 105:1103. [PubMed: 15826011]
3. Ma H, Yip HL, Huang F, Jen AKY. Adv Funct Mater. 2010; 20:1371.
4. DiBenedetto SA, Facchetti A, Ratner MA, Marks TJ. Adv Mater. 2009; 21:1407.
5. Mutin PH, Guerrero G, Vioux A. J Mater Chem. 2005; 15:3761.
6. Layman KA, Hemminger JC. J Catal. 2004; 222:207.
7. Cheng J, Sprik M. J Chem Th & Comp. 2010; 6:880.
8. Luschtinetz R, Frenzel J, Milek T, Seifert G. J Phys Chem C. 2009; 113:5730.
9. Hanson EL, Schwartz J, Nickel B, Koch N, Danisman MF. J Amer Chem Soc. 2003; 125:16074. [PubMed: 14677999]
10. Mutin PH, Lafond V, Popa AF, Granier M, Markey L, Dereux A. Chem Mater. 2004; 16:5670.
11. Nie HY, Walzak MJ, McIntyre NS. J Phys Chem B. 2006; 110:21101. [PubMed: 17048932]
12. Nie HY. Anal Chem. 2010; 82:3371. [PubMed: 20349935]
13. Kagan CR, Breen TL, Kosbar LL. Appl Phys Lett. 2001; 79:3536.
14. Hoeben FJM, Jonkheijm P, Meijer EW, Schenning APHJ. Chem Rev. 2005; 105:1491. [PubMed: 15826018]
15. Leung K, Nielsen IMB, Criscenti LJ. J Amer Chem Soc. 2009; 131:18358. [PubMed: 19947602]
16. Dubey M, Weidner T, Gamble LJ, Castner DG. Langmuir. 2010; 26:14747. [PubMed: 20735054]
17. Halik M, Klauk H, Zschieschang U, Schmid G, Dehm C, Schutz M, Maisch S, Effenberger F, Brunnbauer M, Stellacci F. Nature. 2004; 431:963. [PubMed: 15496917]
18. Klauk H, Zschieschang U, Pflaum J, Halik M. Nature. 2007; 445:745. [PubMed: 17301788]
19. Acton O, Ting G, Ma H, Ka JW, Yip HL, Tucker NM, Jen AKY. Adv Mater. 2008; 20:3697.
20. Anthony JE, Facchetti A, Heeney M, Marder SR, Zhan XW. Adv Mater. 2010; 22:3876. [PubMed: 20715063]
21. Sun J, Zhang B, Katz HE. Adv Funct Mater. 2011; 21:29.
22. Briseno AL, Mannsfeld SCB, Ling MM, Liu SH, Tseng RJ, Reese C, Roberts ME, Yang Y, Wudl F, Bao ZN. Nature. 2006; 444:913. [PubMed: 17167482]
23. Zschieschang U, Halik M, Klauk H. Langmuir. 2008; 24:1665. [PubMed: 18198917]
24. Arias AC, MacKenzie JD, McCulloch I, Rivnay J, Salleo A. Chem Rev. 2010; 110:3. [PubMed: 20070114]
25. Hoque E, DeRose JA, Hoffmann P, Mathieu HJ, Bhushan B, Cichomski M. J Chem Phys. 2006; 124:174710. [PubMed: 16689593]
26. Briggman KA, Stephenson JC, Wallace WE, Richter LJ. J Phys Chem B. 2001; 105:2785.
27. Bell GR, Bain CD, Ward RN. J Chem Soc -Faraday Trans. 1996; 92:515.
28. Robertson J. Rep Prog Phys. 2006; 69:327.
29. Herdt GC, Jung DR, Czanderna AW. Prog Sur Sci. 1995; 50:103.
30. Maitani MM, Daniel TA, Cabarcos OM, Allara DL. J Amer Chem Soc. 2009; 131:8016. [PubMed: 19507902]
31. Maisch S, Buckel F, Effenberger F. J Amer Chem Soc. 2005; 127:17315. [PubMed: 16332081]
32. Park SK, Jackson TN, Anthony JE, Mourey DA. Appl Phys Lett. 2007; 91:063514.

33. Wobkenberg PH, Bradley DDC, Kronholm D, Hummelen JC, de Leeuw DM, Cölle M, Anthopoulos TD. Syn Met. 2008; 158:468.

34. Neves BRA, Salmon ME, Russell PE, Troughton EB. Langmuir. 2000; 16:2409.

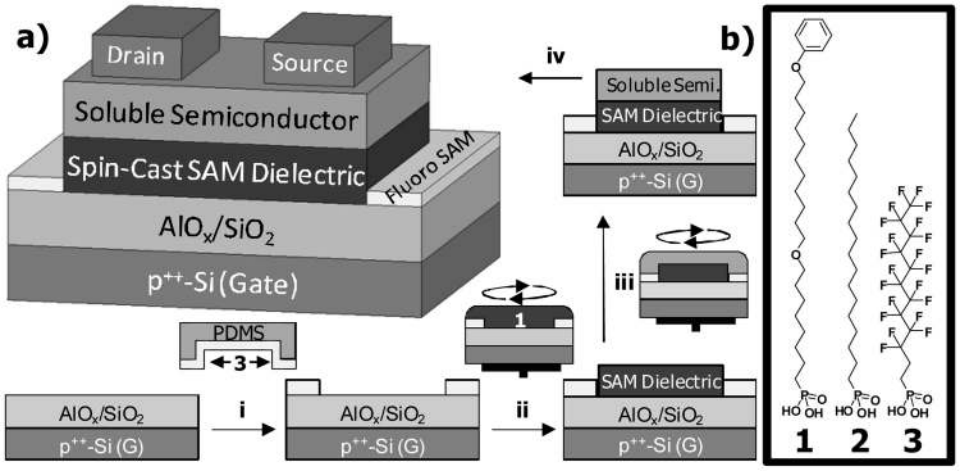

Figure 1.

(a) All-additive fabrication process for spin-cast and patterned SAM dielectric based OTFTs on AlO_x/SiO_2/Si: (i) microcontact printing of **3** on plasma activated AlO_x/SiO_2/Si, (ii) self-organized patterned spin-cast deposition of **1**, (iii) self-organized patterned solution deposition of semiconductor, (iv) thermal evaporation of metal electrodes through shadow mask to complete OTFT device. (b) Structures of PA molecules used in this study. 8-(11-Phenoxy)undecoxyoctylphosphonic acid (**1**), *n*-octadecyl phosphonic acid (**2**), and 1H,1H, 2H,2H-perfluorododecyl-1-phosphonic acid (**3**).

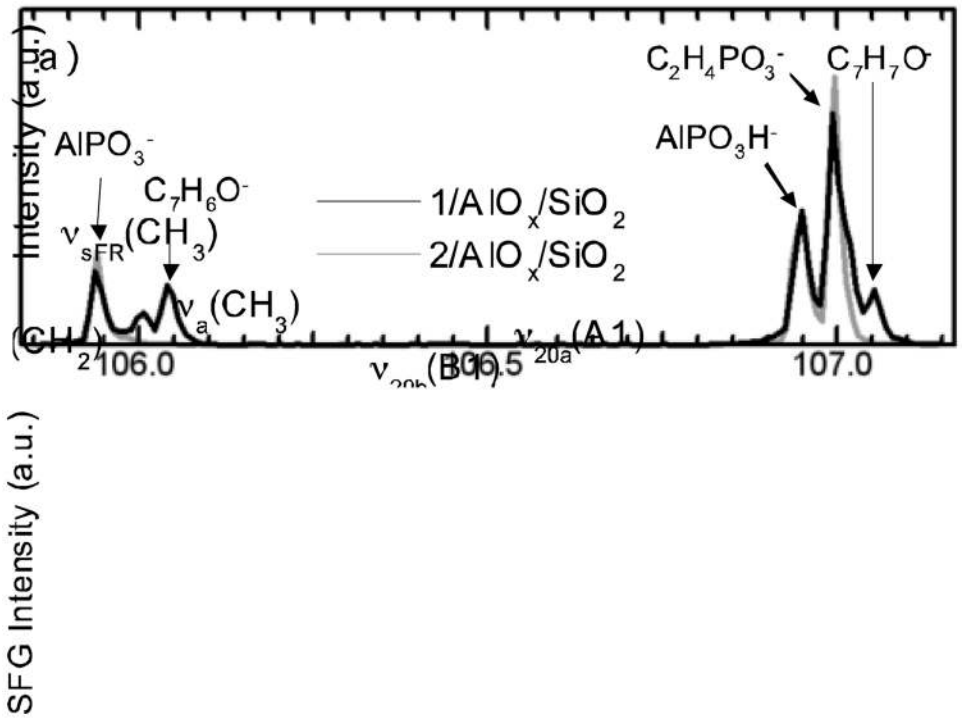

Figure 2.
(a) Negative secondary ion TOF-SIMS data and (b) *ppp* polarization SFG spectra of spin-cast SAMs of **1** and **2** on plasma activated AlO_x/SiO_2.

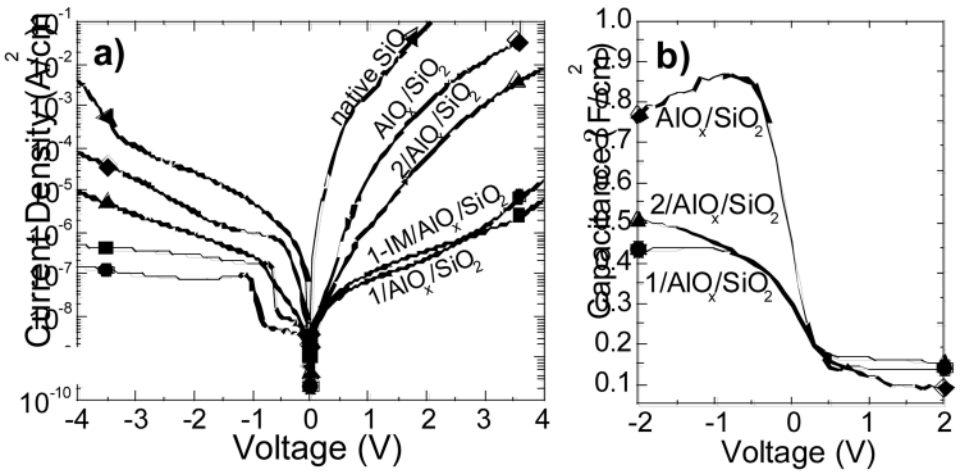

Figure 3.

(a) Leakage current density vs. voltage and (b) capacitance density vs. voltage for spin-cast SAM/ AlO_x/SiO_2 hybrid dielectrics on Si. Also shown is the leakage current density of **1** processed by immersion assembly (1-IM/ AlO_x/SiO_2), plasma grown AlO_x/SiO_2 and native SiO_2.

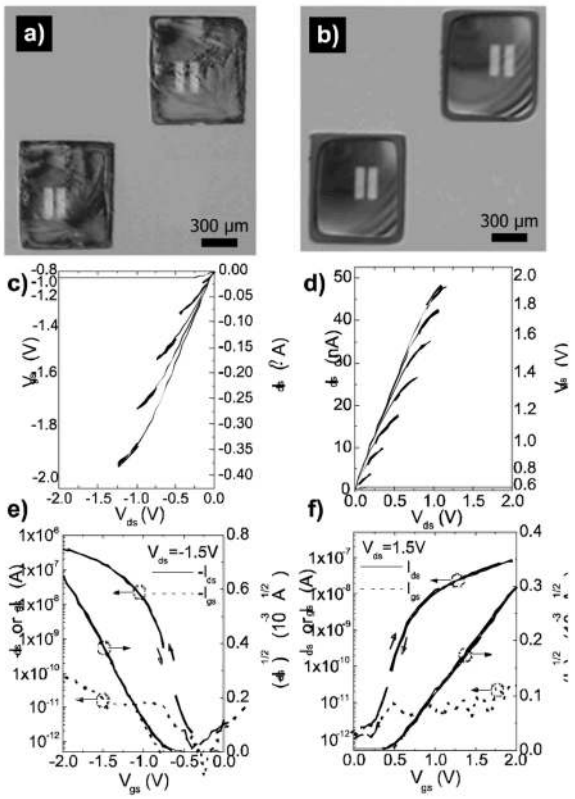

Figure 4.

Optical micrographs (a and b), output (c and d), and transfer (e and f) curve characteristics of low-voltage OTFTs based on spin-cast and patterned SAM hybrid dielectrics of **1** on Si using TIPS-Pen (a, c, and e) and PCBM (b, d, and f) as the semiconductors. (L = 20 □m; W = 200 □m).